Fabrication and temperature-dependent photoluminescence spectra of Zn–Cu–In–S quaternary nanocrystals*

Liu Xiao-Juan(刘晓娟), Zhang Xiao-Song(张晓松)†, Li Lan(李 岚), Wang Xue-Liang(王雪亮), and Yuan Lin-Lin(苑琳琳)

Institute of Material Physics, Tianjin University of Technology, Tianjin 300384, *China*

(Received 21 March 2014; revised manuscript received 9 May 2014; published online 17 September 2014)

A series of Zn–Cu–In–S nanocrystals (ZCIS NCs) are prepared and the optical properties of the ZCIS NCs are tuned by adjusting the reaction time. It is interesting to observe that the temperature-dependent photoluminescence (PL) spectra of the ZCIS NCs show a redshift with decreasing intensity at low temperature (50–280 K) and a blueshift at high temperature (318–403 K). The blueshift can be explained by the thermally active phonon-assisted tunneling from the excited states of the low-energy emission band to the excited states of the high-energy emission band.

Keywords: temperature-dependent photoluminescence, photoluminescence lifetime, quaternary nanocrystals, white light emitting device

PACS: 78.67.Bf, 78.55.–m, 78.40.–q, 78.40.Fy **DOI:** 10.1088/1674-1056/23/11/117804

1. Introduction

Although II–VI and IV–VI group cadmium or lead-based colloidal semiconductor nanocrystals have proven to possess great potential, such as in light emitters, solar cells, and memory devices,[1–4] the intrinsic toxicity of cadmium and lead makes the future applicability of these NCs doubtful.[5–9] In order to find a replacement of these toxic colloidal NCs, which may seriously affect our living environment, groups I–III–VI colloidal NCs, with particular emphasis on $CuInS_2$, have attracted a great deal of attention and investigation.[10,11] In addition, $CuInS_2$ NCs have unique optical properties, which can be controlled through the change of the NC particle size. However, the stability and the emission efficiency of the unmodified $CuInS_2$ NCs are always low. The typical method to improve their photoluminescence quantum yield (PLQY) is Zn doping.[12–14] For example, the emission intensity of Zn–Cu–In–S (ZCIS) NCs was higher than that of $CuInS_2$ NCs, which was reported by Nakamura and co-workers.[15] The PLQY of CZIS NCs synthesized by Xiang *et al.* was up to 70%.[13] Zhang *et al.*[16] fabricated a simple lighting device by using the commercial blue light emitting diode (LED) coated with a CZIS NCs film, the emission wavelength of the device was 580 nm. As a result, the color of the LED was transformed from a cool blue light into a warm yellow light as the LED's emission passed through the NCs film. Later, Zhang *et al.*[17] reported a direct white electroluminescence device, which was obtained in the LEDs by mixing the red emission of ZnCuInS/ZnS core/shell quantum dots (QDs) and the blue-green emission of poly (N, N'-bis (4-butylphenyl)-N, N'-bis (phenyl) benzidine). To better apply the ZCIS NCs to the light emitting devices, it is necessary to investigate the internal luminescence mechanism of the ZCIS NCs. The temperature-dependent PL spectroscopy has been used to study the radiative and the non-radiative relaxation processes as well as the exciton–phonon coupling in colloidal QDs.[18] Therefore, investigating the temperature-dependent optical properties from low to high of luminescent materials for some devices, especially the light emitting devices, has vital significance.[19–23] However, at present the research of ZCIS NCs luminescence mechanism, especially from low to high temperature, is quite rare.

In this paper, the tunable optical properties, the fluorescence decay lifetime at room temperature, and the temperature-dependent PL spectra of ZCIS NCs are respectively investigated. Finally, by combining the ZCIS NCs and an InGaN blue (450 nm) LED, we present a white light emitting device (WLED), and the CIE coordinates are (0.3316, 0.269).

2. Experimental details

2.1. Chemicals

Copper acetate ($Cu(OAc)_2$, 99.99%), indium acetate ($In(OAc)_3$, 99.99%), zinc acetate ($Zn(OAc)_2$, 99.99%), 1-octadecene (ODE, 90%), sulfur powder (99.5%), dodecanethiol (DDT, 98.0%), stearic acid (SA, 99.0%), and octadecylamine (OAm, 98.0%) were purchased from Aldrich. All chemicals were used without further purification.

*Project supported by the National Natural Science Foundation of China (Grand Nos. 60907021, 60977035, and 60877029) and the Natural Science Foundation of Tianjin, China (Grant No. 11JCYBJC00300).

†Corresponding author. E-mail: zhangxiaosong022@126.com

© 2014 Chinese Physical Society and IOP Publishing Ltd

2.2. Precursor solution preparation

$Cu(OAc)_2$/SA/ODE solution: 0.18163 g (1.0 mmol) of $Cu(OAc)_2$, 0.5690 g (2.0 mmol) of SA, and 4.5 mL of ODE were loaded in a three-neck flask clamped in a heating mantle. The mixture was heated to 433 K under an argon flow and remained at this temperature for about 10 min until the formation of a clear deep green solution. The obtained Cu stock solution was stored at 323 K for the following use.

$In(OAc)_3$/SA/ODE: 0.2920 g (1.0 mmol) of $In(OAc)_3$, 1.1380 g (4.0 mmol) of SA, and 4.0 mL of ODE were loaded in a three-neck flask clamped in a heating mantle. The mixture was heated to 473 K under an argon flow and remained at this temperature for about 10 min until the formation of a clear colorless solution. The obtained In stock solution was stored at 323 K for the following use.

$Zn(OAc)_2$/OAm/ODE: 0.5505 g (3.0 mmol) of $Zn(OAc)_2$, 1.940 g of OAm, and 5.5 mL of ODE were loaded in a three-neck flask clamped in a heating mantle. The mixture was heated to 433 K under an argon flow and remained at this temperature for about 10 min until the formation of a clear colorless solution. The obtained Zn stock solution was stored at 323 K for the following use.

S/ODE: 0.0513 g (1.6 mmol) of sulfur dissolved in 4.0 mL of ODE at 393 K, the obtained S stock solution was stored at 323 K for the following use.

2.3. Synthesis of ZCIS NCs

In a typical procedure, the above Cu, In, Zn precursor solutions and 1.0 ml DDT, 3.0 ml ODE were loaded into a 50 mL three-neck flask clamped in a heating mantle. The mixture was heated to 503 K under an argon flow, then the above S precursor solution was injected into the reaction system and kept at this temperature to allow the growth of ZCIS NCs. Aliquots of the sample were taken at different time intervals and injected into cold toluene to terminate the growth of NCs immediately for recording their optical spectra. The obtained ZCIS NCs were precipitated by adding methanol into the toluene solution and purified by repeated centrifugation and decantation.

2.4. Characterization

The phase structure of the sample was investigated by using a Rigaku D/max 2500v/pc X-ray diffractometer with a Cu $K\alpha$ source. The morphology and the size of the sample were characterized by a JEM-2100F transmission electron microscope equipped with a field-emission gun. The absorption spectra were obtained on a Hitachi UV-4100 type ultraviolet–visible–near infrared fluorescence spectrophotometer. The sample was measured under a deuterium light source. The photoluminescence spectra (excitation and emission spectra) were measured by a Jobin Yvon FluoroLog-3 fluorescence spectrometer, and the excitation light sources were a 450-W xenon lamp and a flicker frequency 0.05–25 Hz flashing xenon lamp. The time-correlated single-photon counting (TCSPC) measurements were performed on a Jobin Yvon FluoroLog-3-221-TCSPC fluorescence spectrometer equipped with an EPL456 laser diode.

3. Results and discussion

3.1. Apply the prepared ZCIS NCs for WLED

Figures 1(a) and 1(b) show the transmission electron microscope (TEM) images of the ZCIS NCs prepared with different reaction times. The sizes of the NCs prepared in 30 min and 120 min are about 4.5 ± 0.5 nm and 7.0 ± 0.5 nm, respectively, showing that the sizes of the as-synthesized ZCIS NCs increase with the elevated reaction time. The lattice fringes are clearly observed in the high resolution TEM (HRTEM) images (inset of Fig. 1(a)). The energy dispersive X-ray spectroscopy (EDS) spectrum of the ZCIS NCs prepared in 120 min (Fig. 1(c)) shows that the as-prepared NCs have a quaternary composition, containing Zn, Cu, In, and S. It is identified that the Zn composition of these NCs is 7.29%. Figure 1(d) shows the XRD patterns of the ZCIS NCs. As seen from the figure, the three characteristic peaks are located between the distinct diffraction peaks of $CuInS_2$ (JCPDS 47-1372) and ZnS (JCPDS 65-0309), which indicates the formation of ZCIS quaternary NCs.[13,16] In addition, the full width at half-maximum (FWHM) is observed to decrease with the increasing reaction time, suggesting that the sizes of the NCs increase, which is in line with the analyses of TEM.

Figure 2(a) shows the absorption spectra and the PL emission spectra at room temperature of the ZCIS NCs prepared with a different reaction time excited at 467 nm, and the corresponding emission wavelengths are 621 nm, 646 nm, and 657 nm, respectively, with the increase of the reaction time. Both absorption spectra and emission spectra show obviously a redshift with the increasing reaction time, which can be attributed to the quantum confined effect. The energy band gap for the ZCIS NCs is given by the quantum confinement theory as[24,25]

$$E(R) = E_g + \frac{\hbar^2\pi^2}{2\mu R^2} - \frac{1.786e^2}{\varepsilon R} - 0.248\frac{\mu e^4}{2\varepsilon^2\hbar^2}, \qquad (1)$$

where E_g is the band gap energy of the bulk $CuInS_2$, $\hbar$ is the reduced Planck constant, $\mu = (1/m_e^* + 1/m_h^*)^{-1}$ is the reduced mass of the ZCIS NCs, m_e^* is the effective mass of an electron, m_h^* is the effective mass of a hole, R is the diameter of the nanocrystal, e is the electron charge, and ε is the relative dielectric constant. By using the values of $E_g = 1.53$ eV (for

bulk $CuInS_2$), $m_e^* = 0.16m_0$, $m_h^* = 1.30m_0$,[26] $E(R)$ is calculated based on the absorption spectra at room temperature, the sizes of the ZCIS NCs (R) are calculated as 2.92 nm, 3.75 nm, and 5.13 nm, respectively, which is broadly consistent with the TEM results mentioned above. Therefore, the redshift can be attributed to the quantum confined effect. Figure 2(b) shows the photograph of the samples dispersion in chloroform with a different reaction time taken under the illumination of natural room light. Figure 2(c) shows the photograph of ZCIS NCs samples taken under the illumination of a 450 nm blue LED, and the ZCIS NCs show emission colors ranging from yellow to red under different reaction times. The emission with different wavelength benefits for applications.[13,27–29] A blue LED after being coated with typical ZCIS NCs prepared at the reaction time of 10 min produces white light, as shown in Figs. 2(d) and 2(e). The CIE chromaticity coordinates are shown in Fig. 2(f).

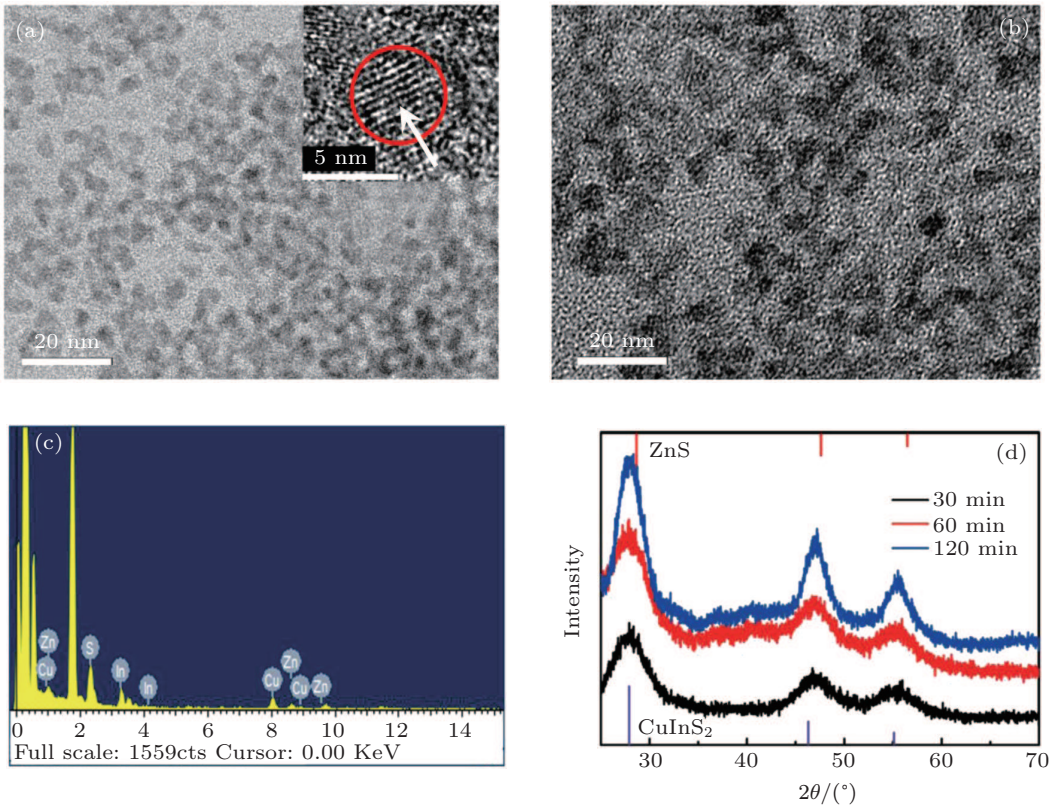


Fig. 1. (color online) TEM images and the corresponding HRTEM images (inset) of ZCIS NCs prepared with the reaction time of (a) 30 min and (b) 120 min. (c) Energy dispersive X-ray spectroscopy spectrum of ZCIS NCs prepared with the reaction time of 120 min. (d) XRD patterns of ZCIS NCs prepared with different reaction times.

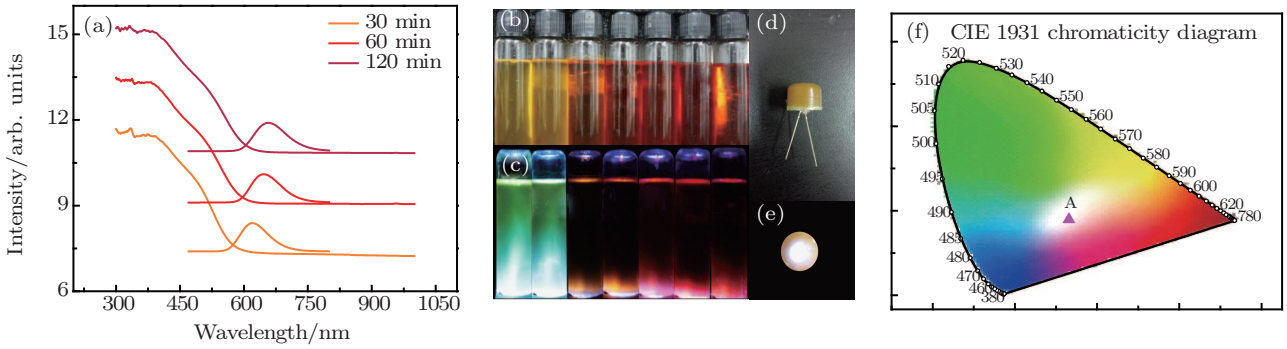


Fig. 2. (color online) (a) Temporal evolution of UV–Vis absorption and PL emission spectra ($\lambda_{ex} = 467$ nm) of ZCIS NCs samples in chloroform solution. (b) Digital photograph of the samples dispersion in chloroform with different reaction times taken under the illumination of natural room light (from left to right: 5 min, 10 min, 20 min, 30 min, 60 min, 90 min, and 120 min). (c) The corresponding photograph of ZCIS NCs samples under the illumination of a 450 nm blue LED. (d) Photograph of an exemplary blue LED after being coated by ZCIS NCs on the surface. (e) The produced white light. (f) CIE chromaticity diagram of ZCIS NCs under the blue light irradiation calculated from the emission spectra.

3.2. PL decay time of ZCIS NCs

To explore the possible luminescence mechanisms involved, the PL decay time of the ZCIS NCs prepared with different reaction times excited by a 456 nm wavelength laser was measured. The PL decays of the ZCIS NCs with reaction times of 20 min, 30 min, and 60 min were detected at the corresponding wavelengths of 596 nm, 621 nm, and 646 nm, respectively, as shown in Fig. 3. The PL decay curves of the ZCIS NCs can be fitted well by a triple-exponential function $I(t) = A_1 \exp(-t/\tau_1) + A_2 \exp(-t/\tau_2) + A_3 \exp(-t/\tau_3)$, where τ_1, τ_2, τ_3 represent the decay time of the PL emission and A_1, A_2, A_3 represent the relative weights of the decay components. The average lifetime τ_{av} is calculated according to $\tau_{av} = \sum A_i \tau_i^2 / \sum A_i \tau_i$.[13] The fitting results are shown in Table 1. The decay time increases with prolonging the reaction time from 20 min to 60 min. As we all known, increasing the reaction time appropriately can provide sufficient time for internal atom assembly and crystalline structure formation, and ultimately minimize the surface defects, thus reducing the fast decay component and increasing the decay time of the ZCIS NCs.

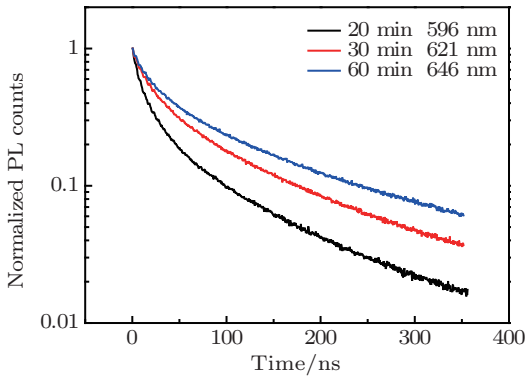


Fig. 3. (color online) PL lifetime decays of ZCIS NCs with different reaction times.

Table 1. Fitting parameters deriving from $I(t) = A_1 \exp(-t/\tau_1) + A_2 \exp(-t/\tau_2) + A_3 \exp(-t/\tau_3)$.

Reaction time	τ_1/ns	A_1/%	τ_2/ns	A_2/%	τ_3/ns	A_3/%	Lifetime/ns
20 min	21.88	25.93	104.7	68.52	5.38	5.55	98.27
30 min	28.55	20.48	122.98	76.27	7.83	3.26	110.40
60 min	730.83	16.24	140.21	81.24	8.05	2.51	135.39

3.3. Temperature dependent photoluminescence of ZCIS NCs

Figure 4(a) shows the temperature-dependent photoluminescence spectra of the ZCIS NCs with the longest lifetime (reaction time 60 min) excited at 395 nm. There have been several reports on the abnormal temperature dependences of luminescence peak position in some semiconductor quantum dots and wells. One of these phenomena is the red-blueshift of the peak energy with increasing temperature.[30–33] In our case, the spectra show redshift at low temperatures from 100 K to 280 K and blueshift at high temperatures from 280 K to 403 K. As can be seen in Fig. 4(b), the peak energy decreases with the increasing temperature at low temperatures, which reveals that NCs PL spectra are strongly dependent on the temperature. The data could be well fitted using the traditional equation introduced by Varshni for the temperature dependence of the band gap[34]

$$E_g(T) = E_g(0) - \frac{\partial T^2}{\beta + T}, \tag{2}$$

where $E_g(0)$ represents the band gap of the ZCIS NCs at 0 K, and ∂ and β are constants. The fitting value of $E_g(0)$ at low temperatures is 2.669 eV, much larger than the band gap of the material at room temperature, 1.83 eV, calculated based on the absorption spectrum at room temperature (see Fig. 4(e)), which is due to the quantum size effect of nanoparticles. The redshift of the band gap may be attributed to the following two factors: (i) the thermal expansion causes a dilation of the lattice with increasing temperature, which results in a change in the band gap energy of the ZCIS NCs; (ii) the major contribution arises from a shift in the relative positions of the conduction and the valence bands due to a temperature dependent electron–phonon interaction.[34,35] This is similar to binary semiconductor NCs; the lattice deformation potential and the exciton–phonon coupling cause a band gap shrinkage, which induces the PL spectral peak redshift with increasing temperature.[36,37] However, the PL spectra of the ZCIS NCs show a blueshift at high temperatures from 280 K to 403 K, which is different from that at low temperatures, as shown in the inset of Fig. 4(b). So the high temperature blueshift cannot be described by Eq. (2). In order to explain the phenomenon, thermally active phonon-assisted tunneling from the excited states of the low-energy emission band to the excited states of the high-energy emission band is introduced in the configuration coordinate diagram. As shown in Fig. 4(c), the thermal back-transfer over the barrier E_2 is possible, and consequently the higher energy emission (EM_1) is dominant at the higher temperature. On the other hand, the barrier E_1 can be overcome and the low-energy emission (EM_2) is dominant at the low temperature. Therefore, the blueshift behavior of the ZCIS NCs is observed with increasing temperature.[19]

As shown in Fig. 4(d), the PL intensity of the ZCIS NCs

decreases significantly when the temperature increases, the excited electrons interact with phonons, and then thermally release through the crossing point between the excited state and the ground state in the configurational coordinate diagram. This nonraditive transition probability by thermal activation is strongly dependent on the temperature, resulting in the decrease of the emission intensity. However, the attenuation trends are not consistent at different temperature ranges. The PL intensity of the ZCIS NCs decreases slowly at low temperatures, while it decreases rapidly at high temperatures. The temperature-dependent intensity can be described by the equation[22,38]

$$I(T) = \frac{I(0)}{1 + A\exp(-\Delta E/kT)}, \tag{3}$$

where T is a thermodynamic temperature, A is a constant, $I(0)$ is the emission intensity at 0 K, k is the Boltzmann constant, and ΔE is the activation energy of the thermal quenching process. The red solid line in Fig. 4(d) is the theoretical fit to the experimental data of low temperature according to Eq. (3) and the fitting results are summarized in Table 2. The activation energy ΔE is 115 meV. In addition, the blue solid line in Fig. 4(d) is the fitting curve at high temperature and the fitting results are summarized in Table 3. The activation energy ΔE is 291 meV. The temperature quenching mechanism of the ZCIS NCs can also be explained by the configuration coordinate as shown in Fig. 4(c), where ΔE_1 represents the activation energy of excited state 1, and ΔE_2 indicates the activation energy of excited state 2. In this case, the activation energy at high temperature is higher than that at low temperature. This probably comes from the surface-related radiative recombination.

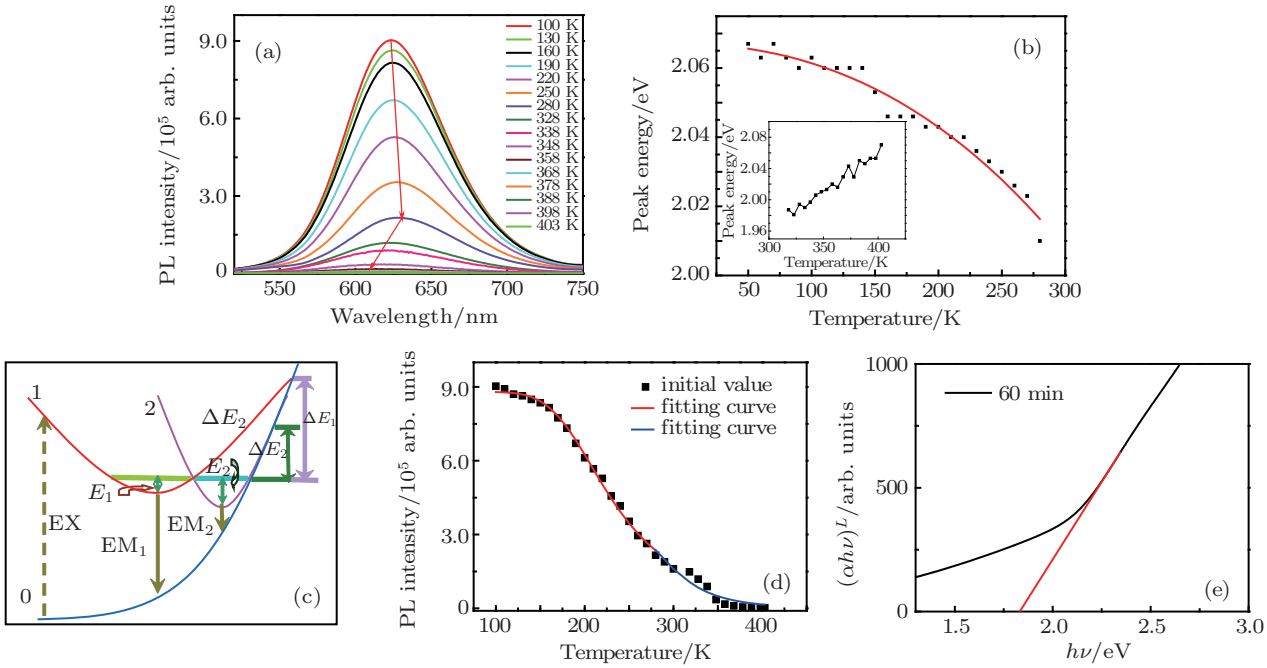


Fig. 4. (color online) (a) Temperature-dependent PL spectra of ZCIS NCs excited at 395 nm from 100 K to 403 K. (b) PL spectral peak energy for ZCIS NCs as a function of temperature, the solid line depicts the best fit of the data in the range of 100–280 K according to Eq. (2), the inset shows the peak energy at high temperature. (c) Configuration coordinate diagram of the ground state 0 and two excited states 1 and 2, showing the energy barrier E_1 for the corresponding transition 1→2 and the energy barrier E_2 for the corresponding transition 2→1. (d) Temperature-dependent PL intensities of ZCIS NCs excited at 395 nm from 100 K to 403 K, the red solid line (left) and the blue solid line (right) are the fitted curves according to Eq. (3). (e) Band gap of ZCIS NCs calculated based on the absorption spectrum at room temperature.

Table 2. Activation energy ΔE of ZCIS NCs at low temperature.

Excitation wavelength/nm	$I(0)$	A	ΔE/eV	Error range of ΔE
395	879552	321	0.115	±0.001

Table 3. Activation energy ΔE of ZCIS NCs at high temperature.

Excitation wavelength/nm	$I(0)$	A	ΔE/eV	Error range of ΔE
395	376718	104168	0.292	±0.001

4. Conclusion

In summary, a series of ZCIS NCs have been prepared and their optical properties are tuned by simply adjusting the reaction time. Our ZCIS NCs can also be used as white LEDs excitied by blue LEDs. In addition, we find the ZCIS NCs fluorescence decay lifetime extended with the increase of the reaction time in the range of 20 min to 60 min. Increasing the reaction time appropriately can provide sufficient time for internal atom assembly and crystalline structure formation.

Moreover, the temperature-dependent PL spectra of the corresponding long decay lifetime material (60 min) show a redshift with increasing temperature from 100 K to 280 K. It can be explained by a dilation of the lattice and a shift in the relative positions of the conduction and the valence bands due to the temperature dependent electron–phonon interaction. The spectra show a blueshift in the range of 280–403 K, which can be explained by back tunneling from the excited states of the low-energy emission band to the excited states of the high-energy emission band with the assistance of thermally active phonons. The spectral intensities of the ZCIS NCs have a temperature quenching effect, and the activation energy ΔE_1 of excited state 1 is lower than the activation energy ΔE_2 of excited state 2. This is probably due to the surface-related radiative recombination.

References

[1] Schlamp M, Peng X G and Alivisatos A 1997 *J. App. Phys.* **82** 5837
[2] Hernández-Borja, Vorobiev Y V and Ramírez-Bon R 2011 *Sol. Energ. Mat. Sol. C* **95** 1882
[3] Li F, Cho S H, Son D I, Park K H and Kim T W 2008 *Appl. Phys. Lett.* **92** 102110
[4] Kannan V and Rhee J K 2012 *Appl. Phys. A* **108** 59
[5] Gardner J S, Shurdha E, Wang C, Lau L D, Rodriguez R G and Pak J J 2007 *J. Nanopart. Res.* **10** 633
[6] Allen P M and Bawendi M G 2008 *J. Am. Chem. Soc.* **130** 9240
[7] Bensebaa F, Durand C, Aouadou A, Scoles L, Du X Wang D and Page Y 2009 *J. Nanopart. Res.* **12** 1897
[8] Pein A, Baghbanzadeh M, Rath T, Haas W, Maier E, Amenitsch H, Hofer F, Kappe C O and Trimmel G 2006 *Chem. Mater.* **18** 3330
[9] Dai M, Ogawa S, Kameyama T, Okazaki K I, Kudo A, Kuwabata S, Tsuboi Y and Torimoto T 2012 *J. Mater. Chem.* **22** 12851
[10] Zhong H Z, Bai Z L and Zou B S 2012 *J. Phys. Chem. Lett.* **3** 3167
[11] Huang S Y, Zhang L D, Li G H, Dai Z H, Zhu X G, Qu F Q, Fu S Q, Zhong Y R and Miao Y 2002 *Chin. Phys. Lett.* **19** 1199
[12] Zhang W J and Zhong X H 2011 *Inorg. Chem.* **50** 4065
[13] Xiang W D, Yang H L, Liang X J, Zhong J S, Wang J, Luo L and Xie C P 2013 *J. Mater. Chem. C* **1** 2014
[14] Liu Y F, Huang F Q, Xie Y, Cui H L, Zhao W, Yang C Y and Dai N 2013 *J. Phys. Chem. C* **117** 10296
[15] Nakamura H, Kato W, Uehara M, Nose K, Omata T, Otsuka-Yao-Matsuo S, Miyazaki M and Maeda H 2006 *Chem. Mater.* **18** 3330
[16] Zhang J, Xie R G and Yang W S 2011 *Chem. Mater.* **23** 3357
[17] Zhang Y, Xie C, Su H P, Liu J, Pickering S, Wang Y Q, Yu W W, Wang J K, Wang Y D, Hahm J I, Dellas N, Mohney S E and Xu J 2011 *Nano Lett.* **11** 329
[18] Liu W Y, Zhang Y, Zhai W W, Wang Y H, Zhang T Q, Gu P F, Chu H R, Zhang H Z, Cui T and Wang Y D 2013 *J. Phys. Chem. C* **117** 19288
[19] Kim J S, Park Y H, Kim S M, Choi J C and Park H L 2005 *Solid State Commun.* **133** 445
[20] Liu B, Shi C S, Zhang Q L and Chen Y H 2002 *J. Alloy. Compd.* **333** 215
[21] Zhang X, Liu Y, Zhi Z, Zhang J, Lu Y, Shen D, Xu W, Fan X and Kong X 2002 *J. Lumin.* **99** 149
[22] Xie R J, Hirosaki N, Kimura N, Sakuma K and Mitomo M 2007 *Appl. Phys. Lett.* **90** 191101
[23] Pejchal J, Nikl M, Mihokova, Novoselov E A, Yoshikawa A and Williams R T 2009 *J. Lumin.* **129** 1857
[24] Brus L E 1983 *J. Chem. Phys.* **79** 5566
[25] Brus L E 1984 *J. Chem. Phys.* **80** 4403
[26] Koc K, Tepehan F Z and Tepehan G G 2011 *Chalcogenide. Lett.* **8** 239
[27] Guo W S, Chen N, Dong C H, Tu Y, Chang J and Zhang B B 2013 *RSC. Adv.* **3** 9470
[28] Wan H K, Ho L M, Whan K T, Yeol Y D and Woo K S 2011 *Appl. Phys. Lett.* **99** 19330.
[29] León-Luis S F, Rodríguez-Mendza U R, Lalla E and Lavín V 2011 *Sensor. Actuat. B Chem.* **158** 208
[30] Zeng H B, Li Z G, Cai W P and Liu P S 2007 *J. Appl. Phys.* **102** 104307
[31] Li Q, Xu S J, Xie M H and Tong S Y 2005 *J. Phys.: Condens. Matter* **17** 4853
[32] Li Q, Xu S J, Cheng W C, Xie M H, Tong S Y, Che C M and Yang H 2001 *Appl. Phys. Lett.* **79** 1810
[33] Xu S J, Li Q, Dong J R and Chua S 2004 *Appl. Phys. Lett.* **84** 2280
[34] Varshni Y P 1967 *Physics* **34** 149
[35] Botha J and Leitch A W R 2000 *J. Electron. Mater.* **29** 1362
[36] Ramvall P, Tanaka S, Nomura S, Riblet P and Aoyagi Y 1999 *Appl. Phys. Lett.* **75** 1935
[37] Wan J, Brebner J, Leonelli R, Zhao G and Graham J 1993 *Phys. Rev. B* **48** 5197
[38] Xu S Y, Zhang X S, Zhou Y L, X Q and Li Lan 2011 *Chin. Phys. Lett.* **20** 037804